# APPENDIX

## A Drag Conductivity

The Kubo approach to frictional drag [95, 89] expresses the drag conductivity $\sigma_{ij}^D(\mathbf{Q},\Omega)$ in terms of a current-current correlation function,

$$\sigma_{ij}^D(\mathbf{Q},\Omega) = \frac{1}{\Omega S}\int_0^\infty dt\, e^{i\Omega t}\left\langle [j_i^{(1)\dagger}(\mathbf{Q},t), j_j^{(2)}(\mathbf{Q},0)]\right\rangle \quad . \tag{A-1}$$

where the indices $i,j$ label the cartesian components of the drag conductivity tensor, $\mathbf{Q}$ and $\Omega$ denote the wave vector and frequency of the applied field, $S$ is the area of the sample, and $j_i^{(l)}$ denotes the $i$th cartesian component of the current operator in the $l$th layer. The dc drag conductivity $\sigma_{ij}^D$ can be obtained from Eq. (A-1) by taking the limit

$$\sigma_{ij}^D = \sigma_{ij}^D(\mathbf{Q}=0,\Omega\to 0) \quad . \tag{A-2}$$

The Feynman diagrams corresponding to Eq. (A-1) consist of two separate electron loops with a vector (current) vertex on each one of them, coupled only by a screened interlayer interaction line (or multiple interaction lines). When the retarded correlation function appearing in Eq. (A-1) is computed within the Matsubara formalism, the leading-order diagrams in the limit of weak (screened) interlayer interaction $U(\mathbf{q},\omega)$ are shown in Fig. A1 (note that the first order diagram with only one internal interaction line does not contribute to the dc drag conductivity we are interested in). Analytically, these diagrams are given by the expression

$$\begin{aligned}\sigma_{ij}^D(i\Omega_k) &= \frac{e^2T}{2\Omega_k S}\sum_{\mathbf{q},\omega_n}\Big\{\Gamma_i^{(1)}(\mathbf{q},i\omega_n+i\Omega_k,i\omega_n)\Gamma_j^{(2)}(\mathbf{q},i\omega_n,i\omega_n+i\Omega_k)\\ &\quad\times U(\mathbf{q},i\omega_n+i\Omega_k)U(\mathbf{q},i\omega_n)\Big\} \quad ,\end{aligned} \tag{A-3}$$

where $T$ is the temperature and $\omega_n$ and $\Omega_k$ denote bosonic Matsubara frequencies

$$\omega_n = 2\pi nT \quad , \qquad \Omega_k = 2\pi kT \quad . \tag{A-4}$$

The prefactor 1/2 in Eq. (A-3) prevents double counting of diagrams. The vector $\mathbf{\Gamma}^{(l)}(\mathbf{q},i\omega_n,i\omega_m)$ stands for the three-leg (or triangle) vertex of layer $l$ as defined by the sum of the two diagrams in Fig. A2. Neglecting *intra*layer interactions, this triangle vertex takes the analytical form

$$\begin{aligned}\mathbf{\Gamma}(\mathbf{q},i\omega_n,i\omega_m) &= T\sum_{\epsilon_k}\mathrm{tr}\Big\{\mathcal{G}(i\epsilon_k)e^{i\mathbf{qr}}\mathcal{G}(i\epsilon_k+i\omega_m)\mathbf{v}\mathcal{G}(i\epsilon_k+i\omega_n)e^{-i\mathbf{qr}}\\ &\quad+\mathcal{G}(i\epsilon_k)e^{-i\mathbf{qr}}\mathcal{G}(i\epsilon_k-i\omega_n)\mathbf{v}\mathcal{G}(i\epsilon_k-i\omega_m)e^{i\mathbf{qr}}\Big\}.\end{aligned} \tag{A-5}$$

Here, $\mathcal{G}$ denotes the electron Green function (for a particular realization of the disorder potential), $\epsilon_k$ is a fermionic Matsubara frequency, and $\mathbf{v}$ represents

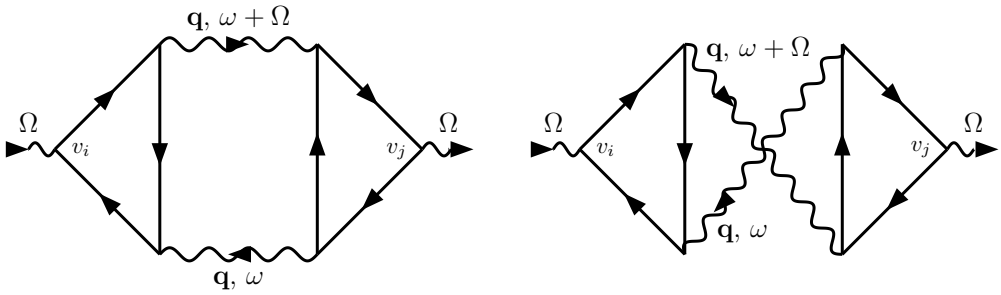


**Figure A1:** The diagrams contributing to the drag conductivity to leading order in the interlayer interaction $U(\mathbf{q},\omega)$ (wavy lines). The straight lines represent the electron Green function. The external vertices, labeled by the velocity operator $v_i$, are vector (current) vertices while the internal vertices are scalar (density) vertices. This figure has been taken from Ref. [86].

the velocity operator. The vertex $\mathbf{\Gamma}$ has to be disorder-averaged, as will be discussed in Appendix D.

For the sake of brevity, from now on we will use the following short-hand notation

$$\mathbf{\Gamma}(\mathbf{q},\omega) \equiv \mathbf{\Gamma}(\mathbf{q},\omega+i0,\omega-i0) \quad .$$

The triangle vertex $\mathbf{\Gamma}(\mathbf{q},\omega)$ can be obtained by analytical continuation of Eq. (A-5), as will be discussed in Appendix C.

Summing over the Matsubara frequency $\omega_n$, performing the analytical continuation to a real frequency $\Omega$, and finally taking the limit $\Omega \to 0$ yields for the dc drag conductivity [95, 89]

$$\sigma_{ij}^{D} = \frac{e^2}{16\pi TS}\sum_{\mathbf{q}}\int_{-\infty}^{\infty}\frac{d\omega}{\sinh^2\left(\frac{\omega}{2T}\right)}\Big\{\Gamma_i^{(1)}(\mathbf{q},\omega+i0,\omega-i0) \times \Gamma_j^{(2)}(\mathbf{q},\omega-i0,\omega+i0)|U(\mathbf{q},\omega)|^2\Big\} \quad . \tag{A-6}$$

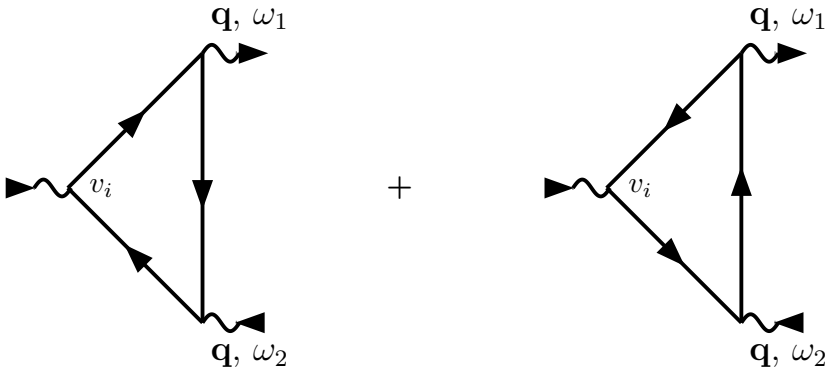


**Figure A2:** Diagrams defining the three-leg triangle vertex $\mathbf{\Gamma}(\mathbf{q},\omega_1,\omega_2)$. As in Fig. A1, the vector (current) vertices are labeled by the velocity operator $v_i$. This figure has been taken from Ref. [86].

This analytical continuation will be performed in Appendix B. Note that the Onsager relation [103]

$$\sigma_{ij}^{12}(B) = \sigma_{ji}^{21}(-B)$$

implies, in combination with Eq. (A-6), that

$$\mathbf{\Gamma}(\mathbf{q}, \omega - i0, \omega + i0; B) = \mathbf{\Gamma}(\mathbf{q}, \omega + i0, \omega - i0; -B) \quad . \tag{A-7}$$

# B Analytical Continuation of the Drag Conductivity

This appendix is devoted to the analytical continuation of the Matsubara expression for the drag conductivity. To calculate the sum over the bosonic Matsubara frequencies $\omega_n = 2\pi nT$ in Eq. (A-3), one performs the standard contour integration in the complex $\omega$ plane,

$$T\sum_{\omega_n} f(i\omega_n) = \frac{1}{4\pi i}\int_{C_b} d\omega\ f(\omega)\ \coth\left(\frac{\omega}{2T}\right) \quad , \tag{B-1}$$

along the integration contour $C_b$ depicted in Fig. B1. The integrand having branch cuts at Im $\omega = 0$ and Im $\omega = -\Omega_k$, where $\Omega_k$ represents the external frequency, the integration contour $C_b$ consists of three parts. Deforming the contour as shown in Fig. B1, one obtains four terms corresponding to the four lines (above and below both branch cuts) forming the new contour $C_b'$, so that

$$\begin{aligned}
\sigma_{ij}^{D}(i\Omega_k) &= -\frac{e^2}{8\pi\Omega_k S}\sum_{\mathbf{q}}\int_{-\infty}^{\infty} d\omega\ \coth\left(\frac{\omega}{2T}\right) \\
&\times \Big\{\Gamma_i^{(1)}(\mathbf{q},\omega+i\Omega_k,\omega+i0)\Gamma_j^{(2)}(\mathbf{q},\omega+i0,\omega+i\Omega_k) \\
&\quad U(\mathbf{q},\omega+i\Omega_k)U(\mathbf{q},\omega+i0) \\
&- \Gamma_i^{(1)}(\mathbf{q},\omega+i\Omega_k,\omega-i0)\Gamma_j^{(2)}(\mathbf{q},\omega-i0,\omega+i\Omega_k) \\
&\quad U(\mathbf{q},\omega+i\Omega_k)U(\mathbf{q},\omega-i0) \\
&+ \Gamma_i^{(1)}(\mathbf{q},\omega+i0,\omega-i\Omega_k)\Gamma_j^{(2)}(\mathbf{q},\omega-i\Omega_k,\omega+i0) \\
&\quad U(\mathbf{q},\omega+i0)U(\mathbf{q},\omega-i\Omega_k) \\
&- \Gamma_i^{(1)}(\mathbf{q},\omega-i0,\omega-i\Omega_k)\Gamma_j^{(2)}(\mathbf{q},\omega-i\Omega_k,\omega-i0) \\
&\quad U(\mathbf{q},\omega-i0)U(\mathbf{q},\omega-i\Omega_k)\Big\} \quad .
\end{aligned} \tag{B-2}$$

In the third and fourth terms, use was made of the fact that

$$\coth\left(z + i\frac{\Omega_k}{2T}\right) = \coth(z) \quad .$$

The contributions due to the points $\omega = 0$ and $\omega = -i\Omega_k$ exactly cancel the integral over the small circles around these points (see Fig. B1). The above integrals should therefore be understood in the principal value sense.

We now present the analytical continuation for the external frequency,

$$i\Omega_k \to \Omega + i0$$

and finally take the limit $\Omega \to 0$ required for a dc external field. As shown in Ref. [95], the first term and the last term (coming from the outer sides of the branch cuts) vanish in the limit $\Omega \to 0$. Using

$$\frac{\partial}{\partial\omega} f(\omega) = \lim_{\Omega\to 0}\frac{f(\omega+\Omega) - f(\omega)}{\Omega} \quad , \tag{B-3}$$

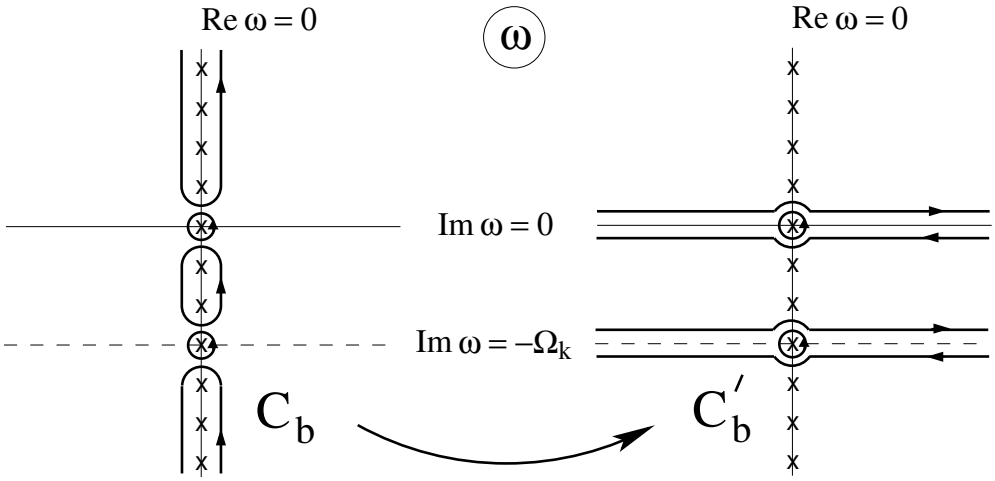


**Figure B1:** Contours for the $\omega$-integration involved in the analytical continuation of the drag conductivity. The left panel shows the original integration contour $C_b$, while the right panel shows the deformation of this contour into a new one, $C_b'$, consisting of two lines on both sides of each of the two branch cuts, as outlined in more detail in the main text. This figure has been taken from Ref. [86].

the remaining nonvanishing terms yield for the dc drag conductivity

$$\begin{aligned}\sigma_{ij}^{D} &= -\frac{e^2}{8\pi S}\sum_{\mathbf{q}}\int_{-\infty}^{\infty} d\omega\ \coth\left(\frac{\omega}{2T}\right)\frac{\partial}{\partial\omega} \\ &\quad\times\Big\{\Gamma_i^{(1)}(\mathbf{q},\omega+i0,\omega-i0)\Gamma_j^{(2)}(\mathbf{q},\omega-i0,\omega+i0) \\ &\qquad U(\mathbf{q},\omega+i0)U(\mathbf{q},\omega-i0)\Big\} \quad . \end{aligned} \tag{B-4}$$

With

$$\frac{\partial}{\partial\omega}\coth\left(\frac{\omega}{2T}\right) = -\frac{1}{2T\sinh^2\left(\frac{\omega}{2T}\right)} \quad , \tag{B-5}$$

one obtains the result stated in Eq. (A-6).

# C Analytical Continuation of the Triangle Vertex

The remaining task is the analytical continuation of the triangle vertex $\Gamma$. Starting point is the expression for the triangle vertex in Eq. (A-5). The summation over the fermionic Matsubara energies $\epsilon_k = 2\pi(k+1/2)T$ in Eq. (A-5) is performed by making use of the integral

$$T\sum_{\epsilon_k} f(i\epsilon_k) = \frac{1}{4\pi i}\int_{C_f} d\epsilon f(\epsilon)\ \tanh\left(\frac{\epsilon}{2T}\right) \quad , \tag{C-1}$$

along the contour $C_f$ shown in Fig. C1.

Since the triangle vertex depends on *two* frequencies $i\omega_m$ and $i\omega_n$, the integrand now has *three* branch cuts in the complex $\epsilon$-plane. They are situated at $\mathrm{Im}\ \epsilon = 0$, $\mathrm{Im}\ \epsilon = -\omega_m$ and $\mathrm{Im}\ \epsilon = -\omega_n$. Similarly to the case of the analytical continuation of the drag conductivity along the contour $C_b$ (see Appendix B), the contour $C_f$ can be deformed into a set of six lines, one on every side of each of the three branch cuts, as depicted in Fig. C1. Performing this deformation of the integration contour, one finds

$$\begin{aligned}
\mathbf{\Gamma}(\mathbf{q}, i\omega_m, i\omega_n) &= \int_{-\infty}^{\infty}\frac{d\epsilon}{4\pi i}\tanh\left(\frac{\epsilon}{2T}\right) \\
&\times \ \mathrm{tr}\left\{\mathbf{v}\ [\mathcal{G}^+(\epsilon)-\mathcal{G}^-(\epsilon)]e^{i\mathbf{qr}}\mathcal{G}(\epsilon-i\omega_n)e^{-i\mathbf{qr}}\mathcal{G}(\epsilon+i\omega_m-i\omega_n)\right. \\
&- \ \mathbf{v}\ \mathcal{G}(\epsilon+i\omega_n)e^{i\mathbf{qr}}[\mathcal{G}^+(\epsilon)-\mathcal{G}^-(\epsilon)]e^{-i\mathbf{qr}}\mathcal{G}(\epsilon+i\omega_m) \\
&+ \ \left.\mathbf{v}\ \mathcal{G}(\epsilon-i\omega_m+i\omega_n)e^{i\mathbf{qr}}\mathcal{G}(\epsilon-i\omega_m)e^{-i\mathbf{qr}}[\mathcal{G}^+(\epsilon)-\mathcal{G}^-(\epsilon)]\right\} \\
&+ \ (\omega_n\to-\omega_m, \mathbf{q}\to-\mathbf{q}) \quad .
\end{aligned} \tag{C-2}$$

In this formula, we use the shorthand notation $\mathcal{G}^{\pm}(\epsilon) = \mathcal{G}(\epsilon \pm i0)$ for the advanced and retarded Matsubara Green functions. In addition, use was made of

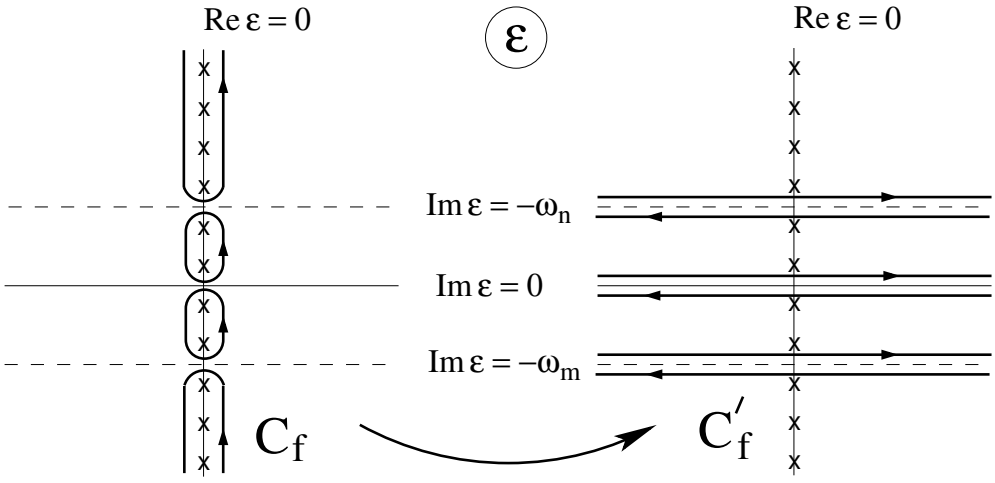


**Figure C1:** Contours for the $\epsilon$-integration involved in the analytical continuation of the triangle vertex. The deformed contour, shown at right side of this figure, consists of lines at both sides of each of the three branch cuts. This figure has been taken from Ref. [86].

the fact that

$$\tanh\left(z - i\frac{\omega_m}{2T}\right) = \tanh\left(z - i\frac{\omega_n}{2T}\right) = \tanh(z) \quad .$$

Although Fig. C1 depicts a specific case regarding the ordering of $\omega_m$, $\omega_n$, and 0, Eq. (C-2) is valid irrespective of the relation between $\omega_m$, $\omega_n$, and 0. Performing the analytical continuation to real frequencies $i\omega_m \to \omega_1 + i0$ and $i\omega_n \to \omega_2 - i0$ (and shifting the integration variables $\epsilon \to \epsilon + \omega_2$ and $\epsilon \to \epsilon + \omega_1$ in the first and third terms, respectively) one obtains

$$\begin{aligned}
\mathbf{\Gamma}(\mathbf{q}, \omega_1 + i0, \omega_2 - i0) \;=\; & \int_{-\infty}^{\infty} \frac{d\epsilon}{4\pi i} \\
& \mathrm{tr}\Bigg\{ \tanh\left(\frac{\epsilon+\omega_2}{2T}\right) \; \mathbf{v} \; [\mathcal{G}^+(\epsilon+\omega_2) - \mathcal{G}^-(\epsilon+\omega_2)] \\
& \quad \times \; e^{i\mathbf{qr}}\mathcal{G}^+(\epsilon) e^{-i\mathbf{qr}}\mathcal{G}^+(\epsilon+\omega_1) \\
& \quad - \; \tanh\left(\frac{\epsilon}{2T}\right) \; \mathbf{v} \; \mathcal{G}^-(\epsilon+\omega_2) e^{i\mathbf{qr}}[\mathcal{G}^+(\epsilon) - \mathcal{G}^-(\epsilon)] \\
& \quad \times \; e^{-i\mathbf{qr}}\mathcal{G}^+(\epsilon+\omega_1) \\
& \quad + \; \tanh\left(\frac{\epsilon+\omega_1}{2T}\right) \mathbf{v} \; \mathcal{G}^-(\epsilon+\omega_2) e^{i\mathbf{qr}}\mathcal{G}^-(\epsilon) \\
& \quad \times \; e^{-i\mathbf{qr}}[\mathcal{G}^+(\epsilon+\omega_1) - \mathcal{G}^-(\epsilon+\omega_1)] \Bigg\} \\
& + (\omega, \mathbf{q} \to -\omega, -\mathbf{q}) \quad . \qquad \text{(C-3)}
\end{aligned}$$

The result of the analytical continuation for the triangle vertex can be written as

$$\mathbf{\Gamma} = \mathbf{\Gamma}^{(a)} + \mathbf{\Gamma}^{(b)} \quad . \qquad \text{(C-4)}$$

Setting $\omega_1 = \omega_2$ (as prescribed by energy conservation) and collecting the contributions containing either only retarded (from the first term) or only advanced (from the third term) Green functions, one arrives (up to a redefinition of the zero of fermionic energies, which are counted from the chemical potential $\mu$ (or $E_F$) in Eq. (C-3)) at the following expression for the contribution $\mathbf{\Gamma}^{(a)}$:

$$\begin{aligned}
\mathbf{\Gamma}^{(a)}(\mathbf{q}, \omega) \;=\; & \int \frac{d\epsilon}{4\pi i} \tanh\left(\frac{\epsilon+\omega-\mu}{2T}\right) \\
& \times \mathrm{tr}\Big\{ \mathbf{v}\mathcal{G}^+(\epsilon+\omega) e^{i\mathbf{qr}}\mathcal{G}^+(\epsilon) e^{-i\mathbf{qr}}\mathcal{G}^+(\epsilon+\omega) \\
& \quad - \mathbf{v}\mathcal{G}^-(\epsilon+\omega) e^{i\mathbf{qr}}\mathcal{G}^-(\epsilon) e^{-i\mathbf{qr}}\mathcal{G}^-(\epsilon+\omega) \Big\} \\
& + (\omega, \mathbf{q} \to -\omega, -\mathbf{q}) \quad , \qquad \text{(C-5)}
\end{aligned}$$

The remaining terms constitute the contribution $\mathbf{\Gamma}^{(b)}$, which can be expressed as

$$\begin{aligned}
\mathbf{\Gamma}^{(b)}(\mathbf{q}, \omega) = & \int \frac{d\epsilon}{4\pi i} \left[ \tanh\left(\frac{\epsilon+\omega-\mu}{2T}\right) - \tanh\left(\frac{\epsilon-\mu}{2T}\right) \right] \\
& \times \mathrm{tr}\left\{ \mathbf{v}\mathcal{G}^-(\epsilon+\omega) e^{i\mathbf{qr}}[\mathcal{G}^-(\epsilon) - \mathcal{G}^+(\epsilon)] e^{-i\mathbf{qr}}\mathcal{G}^+(\epsilon+\omega) \right\} \\
& + (\omega, \mathbf{q} \to -\omega, -\mathbf{q}) \quad . \qquad \text{(C-6)}
\end{aligned}$$

Note that at zero magnetic field only $\mathbf{\Gamma}^{(b)}$ survives [95], whereas $\mathbf{\Gamma}^{(a)}$ containing products of three advanced or three retarded Green functions is zero. By contrast, in finite magnetic fields, both $\mathbf{\Gamma}^{(a)}$ and $\mathbf{\Gamma}^{(b)}$ must be retained. Most importantly, as demonstrated in Chapter 7, there is a cancellation between $\mathbf{\Gamma}^{(a)}$ and $\mathbf{\Gamma}^{(b)}$ to leading order in the ballistic limit.

For small $\omega$, the expressions for $\mathbf{\Gamma}(\mathbf{q},\omega)$ simplify to

$$\mathbf{\Gamma}^{(a)}(\mathbf{q},\omega) = \frac{\omega}{2\pi i}\mathrm{tr}\left\{\mathbf{v}\mathcal{G}^{+}(\mu)e^{i\mathbf{qr}}\mathcal{G}^{+}(\mu)e^{-i\mathbf{qr}}\mathcal{G}^{+}(\mu) - (\mathcal{G}^{+}\rightarrow\mathcal{G}^{-})\right\} \quad \text{(C-7)}$$

$$\mathbf{\Gamma}^{(b)}(\mathbf{q},\omega) = \frac{\omega}{i\pi}\mathrm{tr}\left\{\mathbf{v}\mathcal{G}^{-}(\mu)e^{i\mathbf{qr}}[\mathcal{G}^{-}(\mu)-\mathcal{G}^{+}(\mu)]e^{-i\mathbf{qr}}\mathcal{G}^{+}(\mu)\right\} \quad . \quad \text{(C-8)}$$

For well-separated LLs, this approximation holds as long as $\omega$ is small compared to the width $\Delta$ of the LL. It is also useful to note that $\mathbf{\Gamma}^{(a)}(\mathbf{q},\omega)$ can be expressed as

$$\mathbf{\Gamma}^{(a)}(\mathbf{q},\omega) = \frac{\omega}{\pi}\nabla_{\mathbf{q}}\mathrm{Im}\,\mathrm{tr}\left\{e^{i\mathbf{qr}}\mathcal{G}^{+}(\mu)e^{-i\mathbf{qr}}\mathcal{G}^{+}(\mu)\right\} \quad , \quad \text{(C-9)}$$

which shows that $\mathbf{\Gamma}^{(a)}(\mathbf{q},\omega)$ is a purely longitudinal contribution (i.e., parallel to $\mathbf{q}$) to $\mathbf{\Gamma}(\mathbf{q},\omega)$.

# D Impurity Diagram Technique in High Landau Levels: SCBA

In this appendix, we review the averaging over the random impurity potential $U(\mathbf{r})$. We assume white-noise disorder, characterized by zero mean,

$$\langle U(\mathbf{r})\rangle = 0 \quad , \tag{D-1}$$

and by the correlator

$$\langle U(\mathbf{r})U(\mathbf{r}')\rangle = \frac{1}{2\pi\nu_0\tau_0}\delta(\mathbf{r}-\mathbf{r}') \quad , \tag{D-2}$$

where $\tau_0$ is the elastic scattering time at zero magnetic field and

$$\nu_0 = \frac{m}{2\pi} \tag{D-3}$$

denotes the density of states per spin at zero magnetic field. The assumption of white-noise disorder is certainly unrealistic, since in experiment the disorder potential is correlated on a scale of the order of the distance of the 2DEG layer from the donor layer (typically $\sim 100$ nm), leading to a finite correlation length. However, the results obtained by including realistic smooth disorder with a finite correlation length can be expected to yield results which are qualitatively similar to the results obtained assuming white-noise disorder.

The disorder averaging is performed within the self-consistent Born approximation (SCBA). This approximation neglects diagrams with crossing impurity lines, as sketched in Fig. D1.

When the Fermi energy $E_F$ lies in a high LL with LL index $N \gg 1$, the SCBA has been shown to give the leading contribution in the calculation of disorder-averaged Green functions [104]. Within the SCBA for well-separated Landau levels [105], the impurity average of the Green function, denoted by $G^{\pm}(\epsilon)$, is diagonal in the LL basis $|nk\rangle$ in the Landau gauge and takes the form

$$G_n^{\pm}(\epsilon) = \frac{1}{\epsilon - E_n - \Sigma^{\pm}(\epsilon)} \tag{D-4}$$


**Figure D1:** Diagrammatic representation of second-order contributions to the electron self-energy. In the non-crossing or self-consistent Born approximation (SCBA), only diagrams without crossing impurity lines, such as the one labeled $(a)$, are retained, while diagrams with crossing impurity lines, such as the one labeled $(b)$, are neglected.

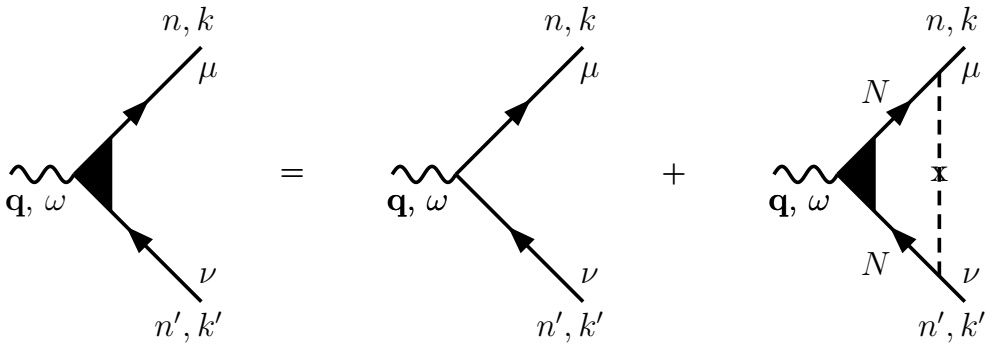


**Figure D2:** Diagrammatic representation of the equation for the vertex corrections $\gamma^{\mu\nu}_{nk,n'k'}(\epsilon+\omega,\epsilon;\mathbf{q})$ (full triangle at vertex) of the scalar (density) vertices within SCBA. Dashed lines represent impurity scattering. For well-separated LLs, it is important to note that the internal Green functions in the rightmost diagram must be evaluated in the valence LL $N$ which, in general, is different from the LL labels $n, n'$ of the external Green functions. This figure has been taken from Ref. [86].

with the LL energy $E_n = \omega_c(n+1/2)$ and the self-energy $\Sigma^{\pm}(\epsilon)$. For energies $\epsilon$ lying within a Landau level ($|\epsilon - E_n| < \Delta$, where $\Delta$ is the LL broadening), this self-energy is given by

$$\Sigma^{\pm}_n(\epsilon) = \frac{1}{2}\left\{\epsilon - E_n \pm i[\Delta^2 - (\epsilon - E_n)^2]^{1/2}\right\} \quad . \tag{D-5}$$

Within the SCBA, the LL broadening $\Delta$ can be expressed in terms of the zero-field scattering time $\tau_0$ as

$$\Delta^2 = \frac{2\omega_c}{\pi\tau_0} \quad . \tag{D-6}$$

The density of states within the SCBA is given by

$$\nu(\epsilon) = \frac{1}{\pi^2\ell_B^2\Delta^2\tau(\epsilon)} = \nu_0\tau_0[\Delta^2 - (\epsilon - E_n)^2]^{1/2} \quad , \tag{D-7}$$

where $\ell_B = (1/eB)^{1/2}$ is the magnetic length and $\tau(\epsilon)$ denotes the elastic scattering time

$$\tau(\epsilon) = [\Delta^2 - (\epsilon - E_n)^2]^{-1/2} \quad . \tag{D-8}$$

In principle, disorder leads to vertex corrections of both the vector and the scalar vertices of the triangle diagram $\mathbf{\Gamma}$. However, for white-noise disorder there are no vertex corrections of the vector vertex. As shown in Fig. D2, the vertex corrections of the scalar vertices generally involve impurity ladders and turn out to be independent of the LL indices $n$ and $n'$,

$$\gamma^{\mu\nu}_{nk,n'k'}(\epsilon+\omega,\epsilon;\mathbf{q}) = \gamma^{\mu\nu}(\mathbf{q},\omega)\,\langle nk|e^{i\mathbf{qr}}|n'k'\rangle \quad . \tag{D-9}$$

The indices $\mu, \nu = \pm$ indicate the type of Green functions involved in the vertex.

In the limit of well-separated Landau levels, explicit expressions for these vertex corrections can be found within the SCBA. We start by noting that

in real space, the impurity-averaged electron Green function in SCBA can be written as

$$G(\mathbf{r},\mathbf{r}';E) = e^{i\varphi(\mathbf{r},\mathbf{r}')}\sum_n C_n(\mathbf{r}-\mathbf{r}')G_n(E) \tag{D-10}$$

with

$$C_n(\mathbf{r},\mathbf{r}') = \frac{1}{2\pi\ell_B^2}e^{-\frac{(\mathbf{r}-\mathbf{r}')^2}{2\ell_B^2}}L_n\left(\frac{(\mathbf{r}-\mathbf{r}')^2}{2\ell_B^2}\right) \quad , \tag{D-11}$$

where $L_n$ is a Laguerre polynomial. The gauge-dependent phase $\varphi(\mathbf{r},\mathbf{r}')$ in Eq. (D-10) satisfies the relation $\varphi(\mathbf{r},\mathbf{r}') = -\varphi(\mathbf{r}',\mathbf{r})$, which can be used to express the vertex correction in real space self-consistently as (see Fig. D2)

$$\begin{aligned}\gamma^{\mu\nu}(\mathbf{q},\omega;\mathbf{r}) = \quad & e^{i\mathbf{qr}} + \frac{1}{2\pi\nu_0\tau_0} \\ & \times \int d\mathbf{r}'\gamma^{\mu\nu}(\mathbf{q},\omega;\mathbf{r}')G^{\mu}(\mathbf{r},\mathbf{r}';E+\omega)G^{\nu}(\mathbf{r}',\mathbf{r};E) \quad .\end{aligned} \tag{D-12}$$

For well-separated Landau levels, the valence LL of index $N$ gives the dominant contribution so that

$$\begin{aligned}\gamma^{\mu\nu}(\mathbf{q},\omega;\mathbf{r}) &= e^{i\mathbf{qr}} + \frac{1}{2\pi\nu_0\tau_0}G_N^{\mu}(E+\omega)G_N^{\nu}(E) \\ &\times \int d\mathbf{r}'C_N(\mathbf{r}-\mathbf{r}')C_N(\mathbf{r}'-\mathbf{r})\gamma^{\mu\nu}(\mathbf{q},\omega;\mathbf{r}') \quad .\end{aligned} \tag{D-13}$$

Using the identity

$$\frac{1}{2\pi\nu_0\tau_0} = \frac{(2\pi\ell_B^2)\Delta^2}{4} \quad , \tag{D-14}$$

one finds that

$$\gamma^{\mu\nu}(\mathbf{q},\omega;\mathbf{r}) = \gamma^{\mu\nu}(\mathbf{q},\omega)e^{i\mathbf{qr}} \tag{D-15}$$

with

$$\begin{aligned}\gamma^{\mu\nu}(\mathbf{q},\omega) &= 1 + \frac{(2\pi\ell_B^2)\Delta^2}{4}\gamma^{\mu\nu}(\mathbf{q},\omega)G_N^{\mu}(E+\omega)G_N^{\nu}(E) \\ &\times \int d\mathbf{r}'C_N(\mathbf{r}-\mathbf{r}')C_N(\mathbf{r}'-\mathbf{r})e^{-i\mathbf{q}(\mathbf{r}-\mathbf{r}')} \quad .\end{aligned} \tag{D-16}$$

The integral is equal to

$$\int d\mathbf{r}'C_N(\mathbf{r}-\mathbf{r}')C_N(\mathbf{r}'-\mathbf{r})e^{-i\mathbf{q}(\mathbf{r}-\mathbf{r}')} = \frac{e^{-q^2\ell_B^2}}{2\pi\ell_B^2}\left[L_N\left(\frac{q^2\ell_B^2}{2}\right)\right]^2 . \tag{D-17}$$

Neglecting the frequency-dependence and using the identities

$$G_N^+G_N^- = \frac{4}{\Delta^2} \quad , \tag{D-18}$$

$$G_N^+G_N^+ = \frac{1}{(\Sigma_N^-)^2} \quad , \tag{D-19}$$

one can solve for $\gamma^{\mu\nu}$ and obtain the explicit expression

$$\gamma^{\mu\nu}(\mathbf{q},\omega) \approx \frac{1}{1-\frac{\Delta^2}{4}e^{-q^2\ell_B^2/2}[L_N^0((q\ell_B)^2/2)]^2G_N^{\mu}(\epsilon+\omega)G_N^{\nu}(\epsilon)} \quad . \tag{D-20}$$

We finally collect relevant matrix elements between LL eigenstates $|nk\rangle$ in the Landau gauge $\mathbf{A} = B(0, x)$. The vector vertex involves the matrix elements

$$\langle nk|v_x|n'k'\rangle = \delta_{kk'}\frac{i}{m\ell_B\sqrt{2}}\left\{\sqrt{n}\delta_{n,n'+1} - \sqrt{n+1}\delta_{n,n'-1}\right\} \quad , \quad \text{(D-21)}$$

$$\langle nk|v_y|n'k'\rangle = \delta_{kk'}\frac{1}{m\ell_B\sqrt{2}}\left\{\sqrt{n}\delta_{n,n'+1} + \sqrt{n+1}\delta_{n,n'-1}\right\} \quad . \quad \text{(D-22)}$$

The scalar vertex involves the matrix element ($n \geq n'$)

$$\begin{aligned}\langle nk|e^{i\mathbf{qr}}|n'k'\rangle &= \delta_{q_y,k-k'}\sqrt{\frac{2^{n'-n}n'!}{n!}}\exp\left[-\frac{1}{4}q^2\ell_B^2 - \frac{i}{2}q_x(k+k')\ell_B^2\right] \\ &\times \quad [(q_y + iq_x)\ell_B]^{n-n'}L_{n'}^{n-n'}\left(\frac{q^2\ell_B^2}{2}\right) \quad , \quad \text{(D-23)}\end{aligned}$$

where $L_m^n$ is the associated Laguerre polynomial.[1]

[1] The expression for the matrix element for $n < n'$ can be obtained from Eq. (D-23) by complex conjugation with the replacements $q \to -q$, $nk \leftrightarrow n'k'$.

# E The Electron-Phonon Interaction in Bulk GaAs

Although we are ultimately interested in the phonon-mediated interaction between 2D electrons in different layers of a bilayer system, it is vital to first gain an understanding of the coupling between electrons and phonons in the bulk. Dealing with systems at very low temperatures, we can restrict ourselves to the study of acoustical phonons in the long wavelength limit. The experimentally studied bilayer systems typically are GaAs/AlGaAs systems. GaAs is a polar semiconductor and therefore behaves quite differently from normal nonpolar materials. Unlike in nonpolar semiconductors (e.g. bulk Ge or Si), in the case of a polar semiconductor an additional mechanism, besides the conventional deformation potential (DP) electron-phonon coupling, arises. This *piezoelectric* (PE) electron-phonon coupling is due to the fact that an acoustical phonon induces a polarization field in crystals that lack a center of inversion [106]. This is the case in GaAs, whose diatomic basis is responsible for the absence of a center of inversion. It will be shown that the PE interaction dominates over the DP interaction at low temperatures $T$, while the latter is prevalent at higher temperatures.

The electron-phonon interaction Hamiltonian can be written as

$$H_{ep} = \int d^3r\, V_{ep}(\mathbf{r})\rho(\mathbf{r}) \quad , \tag{E-1}$$

where $V_{ep}(\mathbf{r})$ is the electron-phonon interaction potential and $\rho(\mathbf{r})$ is the electron density. Delaying a discussion of the specific form of the electron-phonon interaction potential for a moment, we simply assume that it can be expanded into a Fourier series ($V$ is the crystal volume),

$$V_{ep}(\mathbf{r}) = \frac{1}{\sqrt{V}} \sum_{\mathbf{q}} V_{\mathbf{q}} e^{i\mathbf{q}\cdot\mathbf{r}} \quad . \tag{E-2}$$

The electron density also being expanded into a Fourier series,

$$\rho(\mathbf{r}) = \frac{1}{\sqrt{V}} \sum_{\mathbf{p}} \rho_{\mathbf{p}} e^{i\mathbf{p}\cdot\mathbf{r}} \quad , \tag{E-3}$$

the electron-phonon Hamiltonian takes the form

$$H_{ep} = \frac{1}{V} \sum_{\mathbf{pq}} \int d^3r V_{\mathbf{q}} \rho_{\mathbf{p}} e^{i(\mathbf{q}+\mathbf{p})\cdot\mathbf{r}} \tag{E-4}$$

which, after carrying out the integration over $\mathbf{r}$ and the sum over $\mathbf{p}$ leads to

$$H_{ep} = \sum_{\mathbf{q}} V_{\mathbf{q}} \rho_{-\mathbf{q}} \quad . \tag{E-5}$$

Often, the electron-phonon interaction potential is written in the form

$$V_{\mathbf{q}} = \sum_{\lambda} M_{\lambda}(\mathbf{q}) \left[ a_{\lambda}^{\dagger}(-\mathbf{q}) + a_{\lambda}(\mathbf{q}) \right] \quad , \tag{E-6}$$

where $M_{\lambda}(\mathbf{q})$ is the so-called electron-phonon matrix element and $a_{\lambda}^{\dagger}(\mathbf{q})$ ($a_{\lambda}(\mathbf{q})$) are phonon creation (annihilation) operators for phonons of wave vector $\mathbf{q}$ and mode $\lambda$.

## E.1 Phonon Modes

For low-energy excitations, i.e. at sufficiently low temperatures, only the acoustic phonons in the long-wavelength limit are of relevance. In an acoustic wave, the motion of the ions in the basis is synchronous, i.e. the displacement field of the ions varies very slowly on the scale of a Wigner-Seitz cell. Due to the conjoint motion of the basis ions, it is sufficient to consider only the motion of the center of mass of a Wigner-Seitz cell. Throughout this chapter, we therefore assume a monatomic basis of ions of mass $M$, the total mass of a Wigner-Seitz cell, so that there are one longitudinal ($\lambda = 1$ or $l$) and two transverse ($\lambda = 2, 3$ or $t_1, t_2$) phonon modes. Next, we discuss the two relevant types of electron-phonon interaction in a polar semiconductor – deformation potential (DP) and piezoelectric (PE) interaction – and their respective potentials and matrix elements.

## E.2 Deformation Potential Interaction

### Displacement Field

The position of the $n\alpha^{\text{th}}$ ion, i.e. the $\alpha^{\text{th}}$ ion in the $n^{\text{th}}$ elementary cell, can be written as a function of the ionic displacement from its equilibrium position

$$\mathbf{R}_k(t) = \mathbf{R}_{n\alpha} + \mathbf{s}_{n\alpha}(t) \quad . \tag{E-7}$$

The equation of motion for the discrete displacements $\mathbf{s}_n$ in cartesian coordinates (labeled by $i$) is

$$M_\alpha \ddot{s}_{n\alpha i} = -\frac{\partial V}{\partial s_{n\alpha i}} = -\sum_{n',\alpha',i'} \Phi_{n\alpha i}^{n'\alpha' i'} s_{n'\alpha' i'} \quad , \tag{E-8}$$

where $\Phi_{n\alpha i}^{n'\alpha' i'}$ are the atomic force constants which describe the force component in direction $i$ acting upon the $n\alpha^{\text{th}}$ ion when the $n'\alpha'^{\text{th}}$ ion is displaced by unit amount in direction $i'$. Consequently, $\Phi_{n\alpha i}^{n\alpha i} = 0$. The force constants exhibit a large number of symmetries, e.g.

$$\Phi_{n\alpha i}^{n'\alpha' i'} = \Phi_{n'\alpha' i'}^{n\alpha i} \quad , \tag{E-9}$$

which follows from Newton's third principle (actio=reactio). Other symmetries are due to the fact that a translation or a rotation of the crystal as a whole does not cause interatomic forces, or reflect the specific lattice symmetry of the system under consideration.

As mentioned before (Section E.1), for acoustical phonons in the long-wavelength limit both atoms in a diatomic basis oscillate in phase and the oscillation amplitudes vary continuously from elementary cell to elementary cell. Due to the synchronous motion of the atoms in a basis, we restrict our considerations to a simple Bravais lattice of (Wigner-Seitz cell) masses $M$, so that the equation of motion for the discrete $s_{ni}$ of the center of mass of the two ions takes the form

$$M \ddot{s}_{ni} = -\sum_{n'i'} \Phi_{ni}^{n'i'} s_{n'i'} \quad . \tag{E-10}$$

In the continuous limit, a displacement field $\mathbf{s}(\mathbf{r}, t)$ replaces the discrete displacement vectors $\mathbf{s}_n(t)$. Both have to coincide at the discrete points $\mathbf{r} = \mathbf{R}_n$, i.e.

$$\mathbf{s}(\mathbf{r} = \mathbf{R}_n, t) = \mathbf{s}_n(t) \quad . \tag{E-11}$$

The displacement $\mathbf{s}(\mathbf{R}_{n'})$ can now be expanded in a Taylor series around $s(\mathbf{R}_n)$. Up to second order, this yields

$$\begin{aligned} s_{i'}(\mathbf{R}_{n'}) =& s_{i'}(\mathbf{R}_n) + \sum_j \frac{\partial s_{i'}}{\partial r_j} \left(R_{n'j} - R_{nj}\right) \\ &+ \frac{1}{2} \sum_{kl} \frac{\partial^2 s_{i'}}{\partial r_k \partial r_l} \left(R_{n'k} - R_{nk}\right) \left(R_{n'l} - R_{nl}\right) \quad , \end{aligned} \tag{E-12}$$

where it is understood that derivatives are evaluated at the positions $\mathbf{R}_n$. The first two terms lead to vanishing contributions to the equation of motion, so that the leading order is given by the third term alone,

$$M\ddot{s}_{ni} = -\frac{1}{2} \sum_{n'i';kl} \Phi_{0i}^{n'i'} R_{n'k} R_{n'l} \frac{\partial^2 s_{i'}}{\partial r_k \partial r_l} \quad . \tag{E-13}$$

Defining $C_{ii'kl} = \sum_{n'} \Phi_{0i}^{n'i'} R_{n'k} R_{n'l}$ and introducing the mass density $\rho = M/V_{\text{cell}}$, one finds the following equation of motion for the displacement field

$$\rho \ddot{s}_i = \sum_{i'kl} C_{ii'kl} \frac{\partial^2 s_{i'}}{\partial r_k \partial r_l} \quad . \tag{E-14}$$

For a cubic lattice and under the assumption that central forces act between the ions, all indices of $C_{ijkl}$ are interchangeable. The equation of motion can then be written as

$$\rho \ddot{s}_i = \sum_k \sum_{mn} C_{ikmn} \frac{\partial}{\partial r_k} \frac{1}{2} \left( \frac{\partial s_m}{\partial r_n} + \frac{\partial s_n}{\partial r_m} \right) \quad . \tag{E-15}$$

The deformation (or strain) tensor

$$\epsilon_{mn} = \frac{1}{2} \left( \frac{\partial s_m}{\partial r_n} + \frac{\partial s_n}{\partial r_m} \right) \tag{E-16}$$

being related to the stress tensor $\sigma_{ik}$ via Hooke's law,

$$\sigma_{ik} = \sum_{mn} C_{ikmn} \epsilon_{mn} \quad , \tag{E-17}$$

the equation of motion for $\mathbf{s}$ is cast into the form

$$\rho \ddot{s}_i = \sum_k \frac{\partial}{\partial r_k} \sigma_{ik} \quad . \tag{E-18}$$

### Solution of the Equation of Motion

The solutions of the equations of motion, $\mathbf{s}(t)$, are linear combinations of the particular solutions

$$\mathbf{s}_\lambda(\mathbf{q},t) = \frac{1}{\sqrt{NM}}\mathbf{e}_\lambda(\mathbf{q})e^{i(\mathbf{q}\cdot\mathbf{R}_n-\omega_\lambda(\mathbf{q})t)} \tag{E-19}$$

and are given by:

$$s_{\lambda,i}(t) = \frac{1}{\sqrt{NM}}\sum_{\lambda\mathbf{q}} Q_\lambda(\mathbf{q},t)\ \ e_{\lambda,i}(\mathbf{q})\ \ e^{i\mathbf{q}\cdot\mathbf{R}_n} \quad , \tag{E-20}$$

where $M$ is the total mass of a Wigner-Seitz cell (i.e. of a basis), $N$ is the number of Wigner-Seitz cells included in the normalization volume, $Q_\lambda(\mathbf{q},t)$ are the normal coordinates and $e_{\lambda,i}$ is the $i^{\text{th}}$ component of the phonon polarization vector $\mathbf{e}_\lambda(\mathbf{q})$ associated with the frequency $\omega_\lambda(\mathbf{q})$. The polarization vectors $\mathbf{e}_\lambda(\mathbf{q})$ are assumed to be orthonormalized.

### Creation and Annihilation Operators

The phonon creation and annihilation operators are given by

$$a^\dagger_\lambda(\mathbf{q}) = \frac{1}{\sqrt{2\hbar\omega_\lambda(\mathbf{q})}}\left[\omega_\lambda(\mathbf{q})Q^*_\lambda(\mathbf{q}) - iP_\lambda(\mathbf{q})\right] \tag{E-21}$$

and

$$a_\lambda(\mathbf{q}) = \frac{1}{\sqrt{2\hbar\omega_\lambda(\mathbf{q})}}\left[\omega_\lambda(\mathbf{q})Q_\lambda(\mathbf{q}) + iP^*_\lambda(\mathbf{q})\right] \quad , \tag{E-22}$$

where $Q$ and $P$ denote the normal coordinates and the corresponding canonically conjugate momenta. Thus, the normal coordinates can be expressed in terms of these operators via

$$Q_\lambda(\mathbf{q}) = \sqrt{\frac{\hbar}{2\omega_\lambda(\mathbf{q})}}\left[a^\dagger_\lambda(-\mathbf{q}) + a_\lambda(\mathbf{q})\right] \quad . \tag{E-23}$$

### Deformation Potential Approximation

Let $E_C$ be the conduction band energy and $V$ the volume of the crystal. Then, under a dilation of the crystal, the proportionality constant between the relative change of volume and the induced change in conduction band (edge) energy, $\delta E_C$, is called **deformation potential** $D$, namely

$$\delta E_C = D\frac{\delta V}{V} \quad . \tag{E-24}$$

The dependence of the conduction band energy on the displacement field $\mathbf{s}$ can be derived from the equation of continuity,

$$\frac{\partial\rho}{\partial t} + \nabla\cdot\mathbf{j} = 0 \quad , \tag{E-25}$$

using the fact that the (mass) current $\mathbf{j}$ can be expressed in terms of the displacement field $\mathbf{s}$ as

$$\mathbf{j} = \rho \frac{\partial \mathbf{s}}{\partial t} \quad . \tag{E-26}$$

We then find:

$$\delta\rho + \nabla \cdot (\rho \mathbf{s}) = 0 \quad \Rightarrow \quad \nabla \cdot \mathbf{s} = -\frac{\delta\rho}{\rho} = \frac{\delta V}{V} \quad , \tag{E-27}$$

such that

$$\delta E_C = D \nabla \cdot \mathbf{s} \quad . \tag{E-28}$$

The change in conduction band energy is thus proportional to the divergence of $\mathbf{s}$ within this deformation potential approximation [107]. The change of conduction band energy can be interpreted as a potential

$$V(\mathbf{r}) = D \nabla \cdot \mathbf{s} = \frac{D}{\sqrt{V}} \nabla_r \sum_{\mathbf{q}} \mathbf{s}(\mathbf{q}) e^{i\mathbf{q}\cdot\mathbf{r}} = \frac{iD}{\sqrt{V}} \sum_{\mathbf{q}} \mathbf{q} \cdot \mathbf{s}(\mathbf{q}) e^{i\mathbf{q}\cdot\mathbf{r}} \tag{E-29}$$

or

$$V_{\mathbf{q}} = iD\mathbf{q} \cdot \mathbf{s}(\mathbf{q}) \quad . \tag{E-30}$$

In metals, the electron-phonon interaction looks very similar, except that $D$ is to be replaced by a generally nonconstant Fourier component of the electron-ion-potential.

### DP Interaction Matrix Elements

In the deformation potential approximation, the Fourier components of the interaction potential are

$$V_{\mathbf{q}}^{DP} = iD\mathbf{q} \cdot \mathbf{s}_{\mathbf{q}} \quad , \tag{E-31}$$

where $D$ is the deformation potential constant (having dimension of energy) and $\mathbf{s}_{\mathbf{q}}$ is the Fourier component of the displacement. The superscript $DP$ indicates that we are dealing with a deformation potential. Now, $\mathbf{s}_{\mathbf{q}}$ can be expressed as a function of the normal coordinates in the following way

$$\mathbf{s}_{\mathbf{q}} = \frac{1}{\sqrt{MN}} \sum_{\lambda} Q_\lambda(\mathbf{q}) \mathbf{e}_\lambda(\mathbf{q}) \quad , \tag{E-32}$$

where $M$ is the total mass of a Wigner-Seitz cell, $N$ is the number of Wigner-Seitz cells in the crystal, $\mathbf{e}_\lambda(\mathbf{q})$ is the phonon polarization vector of mode $\lambda$ and the normal coordinates $Q_\lambda(\mathbf{q})$ are given by Eq. (E-23). The Fourier components of the potential then take the form

$$V_{\mathbf{q}}^{DP} = \frac{iD}{\sqrt{MN}} \sum_{\lambda} \mathbf{q} \cdot \mathbf{e}_\lambda(\mathbf{q}) Q_\lambda(\mathbf{q}) \tag{E-33}$$

$$= iD \sum_{\lambda} \sqrt{\frac{\hbar}{2\rho V \omega_\lambda(\mathbf{q})}}\, \mathbf{q} \cdot \mathbf{e}_\lambda(\mathbf{q}) \left[ a_\lambda^\dagger(-\mathbf{q}) + a_\lambda(\mathbf{q}) \right] \quad , \tag{E-34}$$

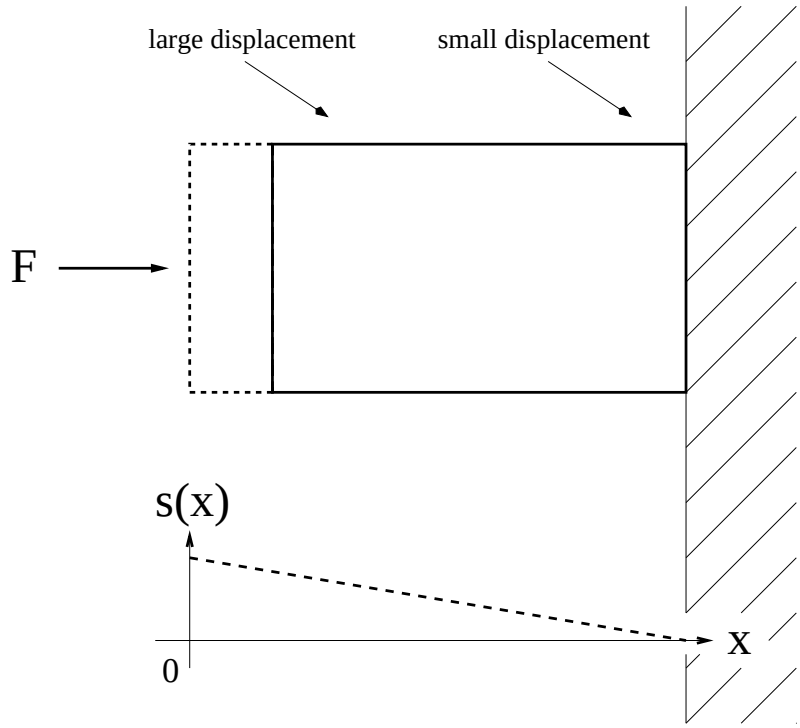


**Figure E1:** Simple picture for piezoelectricity: Under the action of a uniaxial strain caused by a force $F$ in $x$-direction, the volume is deformed into a smaller one. The displacement field $s(x)$ is plotted schematically in the lower part of the figure. Although the displacement varies from large to small values along the $x$-axis, the gradient of the displacement field is constant as can be seen from the constant slope of $s(x)$.

where, in the last step, the ionic mass density $\rho = MN/V$ was introduced. The DP electron-phonon matrix element is

$$M_\lambda^{DP}(\mathbf{q}) = iD\sqrt{\frac{\hbar}{2\rho V\omega_\lambda(\mathbf{q})}}\,\mathbf{q}\cdot\mathbf{e}_\lambda(\mathbf{q}) \quad . \tag{E-35}$$

## E.3 Piezoelectric Interaction

### Piezoelectricity

Piezoelectricity is only present in crystals that lack a center of inversion. Consider an ionic solid like e.g. GaAs with heavy positive (As) and light negative (Ga) ions. In an acoustical phonon mode, all ions tend to vibrate in the *same* direction. However, they need not be displaced by the same amount due to their different masses. If the heavy ions move less than the light ones, a polarization field is induced by the vibrational motion. Roughly, one expects that, upon exerting pressure on a certain volume of the material, the induced polarization $\mathbf{P}$ is proportional to the gradient of the displacement, i.e.

$$\mathbf{P} \propto \nabla s \quad . \tag{E-36}$$

This can be seen easily in Fig. E1: The displacement field $s(x)$ is large at the left side, where the force is applied, while it is small at the right side of the deformed volume. The gradient of the displacement field, however, is constant, i.e. $s(x)$ varies linearly with $x$. The polarization $\mathbf{P}$ is thus proportional to $\nabla s(x)$, not simply $s(x)$. The electron-phonon interaction can be described by a potential $V(x)$ whose gradient is the field $\mathbf{P} = \nabla V(x)$, from which follows that

$$V(x) \propto s(x) \quad .$$

Comparison with the DP interaction, which yields $V_{DP} \propto \nabla \cdot \mathbf{s}$ and thus $V(\mathbf{q}) \propto i\mathbf{q} \cdot \mathbf{s}(\mathbf{q})$, shows that there is an additional factor of $i\mathbf{q}$ in the DP case due to the additional gradient.

More rigorously, the derivation goes as follows. In a non-piezoelectric material, the following relations hold

$$\sigma_{ij} = C_{ijkl}\ \epsilon_{kl} \qquad\qquad D_k = \varepsilon_{ik} E_i \quad , \tag{E-37}$$

where $\sigma_{ij}$ is the stress tensor, $\epsilon_{kl}$ is the deformation or strain tensor, $D_k$ is the dielectric displacement field and $E_i$ is the electric field. The tensors $C_{ijkl}$ and $\varepsilon_{ik}$ (not to be confused with $\epsilon_{kl}$) are the elastic moduli and the dielectric tensor, respectively. The first of the two equations is known as stress-strain-relation. These relations have to be extended in a piezoelectric material to include polarization effects. They then read:

$$\sigma_{ij} = C_{ijkl}\ \epsilon_{kl} - e_{kij} E_k \qquad\qquad D_k = \varepsilon_{ik} E_i + P_k = \varepsilon_{ik} E_i + e_{kij} \epsilon_{ij} \quad . \tag{E-38}$$

The quantity $e_{kij}$ is the so-called piezoelectric tensor. The first of the two equations describes the so-called converse piezoelectric effect, where an electric field induces a mechanical stress. The second equation describes the direct piezoelectric effect, where a mechanical strain produces polarization and therefore (di)electric displacement. Due to the symmetry of stress and strain tensors (which is due to their very definition),

$$\sigma_{ij} = \sigma_{ji} \qquad\qquad \epsilon_{ij} = \epsilon_{ji} \quad , \tag{E-39}$$

there are only six independent elements of $\sigma_{ij}$ and $\epsilon_{ij}$. They can therefore be written as six-component column vectors. The $3^3 = 27$ elements of the third rank piezoelectric tensor $e_{kij}$ thus reduce to $3 \times 6 = 18$ elements and the tensor can be replaced by a $(3 \times 6)$-matrix. The number of independent components is reduced dramatically by the crystal symmetry of GaAs, as will be shown in the next section.

### The PE Tensor of Gallium Arsenide

GaAs has zincblende structure and thus cubic tetragonal symmetry (point group $T_d$ in Schönflies notation or $\bar{4}3m$ in international notation). The absence of a center of inversion renders this material piezoelectric. The transformation matrices for the symmetry group generators are (in international notation)

$$M_8 = \begin{pmatrix} 0 & -1 & 0 \\ 1 & 0 & 0 \\ 0 & 0 & -1 \end{pmatrix} \tag{E-40}$$

and

$$M_{13} = \begin{pmatrix} 0 & 0 & 1 \\ 1 & 0 & 0 \\ 0 & 1 & 0 \end{pmatrix} \quad . \tag{E-41}$$

They correspond to a fourfold inversion-rotation about the 3-axis and a threefold rotation about the [111]-direction, respectively.

The polarization $P_i$ is related to the strain tensor $\epsilon_j$ via[2]

$$P_i = e_{ij}\epsilon_j \quad , \tag{E-42}$$

where $e_{ij}$ is the piezoelectric tensor and $i$ runs from one to three while $j$ runs from one to six, owing to the fact that the symmetry $\epsilon_{lm} = \epsilon_{ml}$ of the strain tensor reduces the number of its independent components to six. The strain tensor is then written as a six-component column vector and the indices $j = 1 \ldots 6$ correspond to $11, 22, 33, 23 = 32, 31 = 13, 12 = 21$ in this order.[3]

The statement we want to prove is that the piezoelectric tensor takes the form

$$e_{ij} = \begin{pmatrix} 0 & 0 & 0 & e_{14} & 0 & 0 \\ 0 & 0 & 0 & 0 & e_{14} & 0 \\ 0 & 0 & 0 & 0 & 0 & e_{14} \end{pmatrix} \quad , \tag{E-43}$$

i.e. that $e_{14} \equiv e_{123} = e_{132} = e_{231} = e_{213} = e_{312} = e_{321} \neq 0$ and all other elements, containing one index at least twice, are zero.

The Neumann principle states that under a symmetry transformation of the crystal, every component of $e_{ij}$ stays invariant (i.e., is transformed into itself). Formally, if under a symmetry transformation (1,2,3 label coordinate axes)

$$\begin{array}{ccc} 1 & \rightarrow & 1' \\ 2 & \rightarrow & 2' \\ 3 & \rightarrow & 3' \end{array} \quad , \tag{E-44}$$

then

$$e_{ijk} = e_{i'j'k'} \tag{E-45}$$

must hold. We have

$$M_8: \quad \begin{array}{ccc} 1 & \rightarrow & -2 \\ 2 & \rightarrow & 1 \\ 3 & \rightarrow & -3 \end{array} \qquad\qquad M_{13}: \quad \begin{array}{ccc} 1 & \rightarrow & 3 \\ 2 & \rightarrow & 1 \\ 3 & \rightarrow & 2 \end{array} \quad . \tag{E-46}$$

The reasoning now proceeds as follows:

- $M_{13}$ directly implies $e_{111} = e_{222} = e_{333}$.

[2] This can be read off directly from the second relation in Eq. (E-38) using the macroscopic electrodynamic relation $\mathbf{D} = \hat{\varepsilon}\mathbf{E} + \mathbf{P}$.

[3] Note that normally, $e_{in}$ is defined by $e_{in} = e_{ijk}$ for $n = 1, 2, 3$ and by $e_{in} = 2e_{ijk}$ for $n = 4, 5, 6$. This assures that the strain tensor, written in vector form, still satisfies the stress-strain relation. If one writes e.g. $e_{kn}\epsilon_n$, each term such as $e_{k4}\epsilon_4$ is counted only once, whereas in $e_{kij}\epsilon_{ij}$, this term would be counted twice. The factor of 2 accounts for this fact. We, in turn, skip this convention and think of $e_{14}$ as one of the components of the third-rank tensor, i.e. $e_{14} = e_{123} = \ldots$

- $M_8$ implies $e_{333} = -e_{333} \Rightarrow e_{333} = 0$.
- Therefore, $e_{111} = e_{222} = e_{333} = 0$.
- From $M_8$ it follows that $e_{112} = e_{221} = -e_{112}$ and thus $e_{112} = 0$. The same holds for all other $e_{iik}, e_{iki}, e_{kii}$ as can be shown by using $M_{13}$ to establish the identity of, e.g., $e_{112} = e_{331} = e_{223}$.
- The remaining six components can be shown to be equal using first $M_{13}$ to establish $e_{123} = e_{312} = e_{231}$ as well as $e_{132} = e_{321} = e_{213}$ and then by using $M_8$ to prove $e_{123} = e_{231}$.
- There exists no relation of the type $e_{ijk} = -e_{ijk}$ for three different indices since every index appears only once and thus the two sign changes occurring under $M_8$ compensate.

We thus have

$$e_{ijk} = \begin{cases} e_{123} \equiv e_{14} & \text{for } i \neq j, j \neq k, i \neq k \\ 0 & \text{else} \end{cases} \quad , \tag{E-47}$$

which is exactly what we wanted to prove. The piezoelectric tensor of GaAs indeed has only one independent entry.

### Piezoelectric Coupling

Consider a single acoustical phonon with wave vector $\mathbf{q}$. This phonon causes a displacement $\mathbf{s}(\mathbf{q})$ and thus a strain field $\epsilon_{ij}(\mathbf{q})$. What is the electric field (or polarization) induced by this field?

As an approximation, we assume the absence of free carriers in the subsequent discussion. From $\nabla \cdot \mathbf{D} = 0$ follows $q_k D_k = 0$, which, using the second relation in Eq. (E-38) yields

$$q_k \left[ e_{k\alpha} \epsilon_\alpha(\mathbf{q}) + \varepsilon_{ki} E_i(\mathbf{q}) \right] = 0 \quad . \tag{E-48}$$

Since $E_i(\mathbf{q})$ is a longitudinal field,

$$E_i(\mathbf{q}) = \frac{q_i}{q} E(\mathbf{q}) \quad , \tag{E-49}$$

we can write

$$E(\mathbf{q}) = -\frac{q q_k e_{k\alpha} \epsilon_\alpha(\mathbf{q})}{q_i \varepsilon_{im}(\mathbf{q}) q_m} \quad . \tag{E-50}$$

Again, due to the fact that $E_i(\mathbf{q})$ is a longitudinal field, we can define a potential $\mathbf{E}(\mathbf{r}) = -\nabla V$ or, equivalently, $\mathbf{E}(\mathbf{q}) = -i\mathbf{q} V_{\mathbf{q}}$ which can be read off from Eq. (E-50) to be

$$V_{\mathbf{q}} = -i \frac{q_k e_{k\alpha} \epsilon_\alpha(\mathbf{q})}{q_i \varepsilon_{im}(\mathbf{q}) q_m} \tag{E-51}$$

### PE Interaction Matrix Elements

The structure of GaAs is cubic, so the dielectric tensor $\varepsilon(\hat{\mathbf{q}})$ is isotropic and we can replace $\varepsilon_{im}(\mathbf{q})$ by the dielectric constant $\varepsilon_0$, which is independent of $\mathbf{q}$ in Eq. (E-51). The piezoelectric interaction thus is described by the potential

$$V_{\mathbf{q}}^{PE} = -i\frac{q_k e_{kij}\epsilon_{ij}(\mathbf{q})}{\varepsilon_0 q^2} \quad , \tag{E-52}$$

where $e_{kij}$ is the piezoelectric tensor, $\epsilon_{ij}(\mathbf{q})$ are the Fourier components of the strain tensor given by

$$\epsilon_{ij}(\mathbf{q}) = \frac{i}{2}\left[q_i s_j(\mathbf{q}) + q_j s_i(\mathbf{q})\right] \tag{E-53}$$

and $\varepsilon_0$ is the dielectric constant.

The potential acting on an electron is given by a summation over *all* phonon modes. At low temperatures, only longitudinal acoustical (LA) and transverse acoustical (TA) modes are present, so we can neglect the longitudinal and transverse optical modes (LO,TO) in this summation. Using again Eq. (E-32) to express $s_{\mathbf{q}} = s(\mathbf{q})$ as a function of the normal coordinates $Q_\lambda$, the interaction potential can be written ($e_{\lambda,i}(\mathbf{q})$ is the $i^{\text{th}}$ cartesian component of the phonon polarization vector)

$$V_{\mathbf{q}}^{PE} = \sum_\lambda \sqrt{\frac{\hbar}{2\rho V\omega_\lambda(\mathbf{q})}}\frac{q_k e_{kij}\left(q_i e_{\lambda,j}(\mathbf{q}) + q_j e_{\lambda,i}(\mathbf{q})\right)}{2q^2\varepsilon_0}\left[a_\lambda^\dagger(-\mathbf{q}) + a_\lambda(\mathbf{q})\right] \tag{E-54}$$

and the matrix element is thus

$$M_\lambda^{PE}(\mathbf{q}) = \sqrt{\frac{\hbar}{2\rho V\omega_\lambda(\mathbf{q})}}\frac{q_k e_{kij}\left(q_i e_{\lambda,j}(\mathbf{q}) + q_j e_{\lambda,i}(\mathbf{q})\right)}{2q^2\varepsilon_0} \quad , \tag{E-55}$$

which can be simplified considerably making again use of the fact that the piezoelectric modulus $e_{kij}$ has only a single independent component $e_{123} \equiv e_{14}$ due to the cubic zincblende structure of GaAs. This reduces the matrix element to

$$M_\lambda^{PE}(\mathbf{q}) = \sqrt{\frac{\hbar}{2\rho V\omega_\lambda(\mathbf{q})}} \quad \frac{2e_{14}}{\varepsilon_0 q^2}\left(q_1 q_2 e_{\lambda,3} + q_1 q_3 e_{\lambda,2} + q_2 q_3 e_{\lambda,1}\right) \quad . \tag{E-56}$$

Further simplifications are possible for specific polarizations $\lambda$. For LA phonons ($\lambda = 1$), the same term appears three times since $\mathbf{q} \parallel \mathbf{e}_1$, because $q_i q_j e_{1,k}/q^2$ is the same for any permutation of $i, j, k$.

## E.4 Long Wavelength Limit and Isotropic Debye Approximation

In the long wavelength limit, the polarization vector $\mathbf{e}_l = \mathbf{e}_1$ of the longitudinal phonons is parallel to $\mathbf{q}$, i.e.

$$\mathbf{e}_l(\mathbf{q}) = \frac{\mathbf{q}}{q} \quad , \tag{E-57}$$

and the polarization vectors $\mathbf{e}_{t_1} = \mathbf{e}_2$, $\mathbf{e}_{t_2} = \mathbf{e}_3$ of the transverse phonons are perpendicular to $\mathbf{q}$. In this limit, only longitudinal phonons interact via DP with electrons due to the factor $\mathbf{q} \cdot \mathbf{e}_\lambda(\mathbf{q})$ in $M_\lambda^{DP}(\mathbf{q})$ of Eq. (E-35). For the longitudinal phonons, this yields for the matrix element

$$M_l^{DP}(\mathbf{q}) = iD\sqrt{\frac{\hbar}{2\rho V \omega_l(\mathbf{q})}}\ \mathbf{q} \cdot \frac{\mathbf{q}}{q} = iDq\sqrt{\frac{\hbar}{2\rho V \omega_l(\mathbf{q})}} \tag{E-58}$$

The isotropic Debye approximation [97, 108] neglects the anisotropy in the speed of sound by setting

$$\omega_\lambda(\mathbf{q}) = c_\lambda q \quad , \tag{E-59}$$

where $c_1 = c_l$, $c_2 = c_3 = c_t$. Upon replacing $\omega_l(\mathbf{q})$ by $c_l q$ in Eq. (E-58), the matrix element $M_l^{DP}(\mathbf{q})$ takes the form

$$M_l^{DP}(\mathbf{q}) = iD\sqrt{\frac{\hbar q}{2\rho V c_l}} \tag{E-60}$$

This matrix element is proportional to $\sqrt{q}$ and independent of the direction of $\mathbf{q}$. As will be shown below, this is in contrast to the PE matrix elements, which depend strongly on the direction of $\mathbf{q}$ rather than on its magnitude. For completeness, we again stress that, in the long wavelength limit,

$$M_{t_1}^{DP}(\mathbf{q}) = M_{t_2}^{DP}(\mathbf{q}) = 0 \quad . \tag{E-61}$$

For the piezoelectric interaction, the isotropic Debye approximation consists in letting $\omega_l(\mathbf{q}) = c_l q$ and $\omega_{t_1}(\mathbf{q}) = \omega_{t_2}(\mathbf{q}) = c_t q$. In the long wavelength limit, $\mathbf{e}_l$ is again given by $\mathbf{e}_l(\mathbf{q}) = \mathbf{q}/q$ and thus

$$M_l^{PE}(\mathbf{q}) = \sqrt{\frac{\hbar}{2\rho V c_l q}}\frac{6e_{14}q_1q_2q_3}{\varepsilon_0 q^3} \tag{E-62}$$

while the transverse matrix elements $M_{t_1,t_2}^{PE}(\mathbf{q})$ are given by

$$M_{t_1}^{PE}(\mathbf{q}) = \sqrt{\frac{\hbar}{2\rho V c_t q}}\frac{2e_{14}}{\varepsilon_0 q^2}\left(q_1q_2e_{t_1,3} + q_1q_3e_{t_1,2} + q_2q_3e_{t_1,1}\right) \tag{E-63}$$

and

$$M_{t_2}^{PE}(\mathbf{q}) = \sqrt{\frac{\hbar}{2\rho V c_t q}}\frac{2e_{14}}{\varepsilon_0 q^2}\left(q_1q_2e_{t_2,3} + q_1q_3e_{t_2,2} + q_2q_3e_{t_2,1}\right) \quad . \tag{E-64}$$

All three PE matrix elements are thus proportional to $\sqrt{1/q}$, so that

$$\frac{M_l^{DP}(\mathbf{q})}{M_\lambda^{PE}(\mathbf{q})} \propto q \quad . \tag{E-65}$$

Furthermore, $M_l^{DP}(\mathbf{q})$ and $M_l^{PE}(\mathbf{q})$ differ by a phase of $\pi/2$ due to the additional factor of $i$ in $M_l^{DP}(\mathbf{q})$ (Eq. (E-60)). In second order processes, as needed

for the determination of an effective electron-electron interaction, there is thus no interference between the DP and PE matrix elements.

Within all the above approximations (deformation potential approximation, monatomic lattice of ions with total mass $M$, long wavelength limit, isotropic Debye approximation), the electron-phonon matrix elements are given by

$$M_l(\mathbf{q}) = M_l^{DP}(\mathbf{q}) + M_l^{PE}(\mathbf{q}) = iD\sqrt{\frac{\hbar q}{2\rho V c_l}} + \sqrt{\frac{\hbar}{2\rho V c_l q}}\frac{6e_{14}q_1q_2q_3}{\varepsilon_0 q^3} \tag{E-66}$$

$$M_{t_1}(\mathbf{q}) = M_{t_1}^{PE}(\mathbf{q}) = \sqrt{\frac{\hbar}{2\rho V c_t q}}\frac{2e_{14}}{\varepsilon_0 q^2}\left(q_1q_2e_{t_2,3} + q_1q_3e_{t_2,2} + q_2q_3e_{t_2,1}\right) \tag{E-67}$$

$$M_{t_2}(\mathbf{q}) = M_{t_2}^{PE}(\mathbf{q}) = \sqrt{\frac{\hbar}{2\rho V c_t q}}\frac{2e_{14}}{\varepsilon_0 q^2}\left(q_1q_2e_{t_2,3} + q_1q_3e_{t_2,2} + q_2q_3e_{t_2,1}\right) \tag{E-68}$$

It is not possible, at this point, to simply add them, because the phonon creation and annihilation operators in the interaction Hamiltonian are mode-specific, i.e. they carry an index $\lambda$, too, which may not be omitted. In the process of deriving the phonon-mediated interlayer interaction (see Chapter 7), there will be an averaging over (in-plane) transverse phonon polarizations that allows us to define a common transverse matrix element.

# F Laguerre Polynomials and Vertex Overlaps

In this Appendix, we review some well-known asymptotic expansions of the generalized Laguerre polynomials [76] used in our derivation of the phonon drag conductivity in Chapter 7 and also derive asymptotic expressions for the vertex overlaps.

## F.1 Asymptotic Expansions of the Generalized Laguerre Polynomials

We need expansions of $e^{-x/2}L_n^\alpha(x)$ for large $n$ or $\alpha$ for three regions of $x$:

(i) $x$ in the vicinity of zero,

(ii) in the oscillatory region,

(iii) in the monotonic region.

For $x$ in the vicinity of zero, $0 \leq x < \nu^{1/3}$, where $\nu = 4n + 2\alpha + 2$, we have

$$e^{-x/2}L_n^\alpha(x) \approx \frac{\Gamma(n+\alpha+1)}{\Gamma(n+1)} \left(\frac{4}{\nu x}\right)^{\frac{\alpha}{2}} J_\alpha\left((\nu x)^{\frac{1}{2}}\right) \quad . \tag{F-1}$$

For the range $0 < x < n^{1/3}$, one can specialize this expansion to Fejér's formula

$$e^{-x/2}L_n^\alpha(x) \approx \frac{\Gamma(n+\alpha+1)}{\Gamma(n+1)} \left(\frac{4}{\nu x}\right)^{\frac{1}{4}+\frac{\alpha}{2}} \cos\left((\nu x)^{\frac{1}{2}} - \alpha\frac{\pi}{2} - \frac{\pi}{4}\right) \quad . \tag{F-2}$$

In the oscillatory region, $x < \nu$, the generalized Laguerre polynomials are given by

$$e^{-x/2}L_n^\alpha(x) \approx (-1)^n \frac{\Gamma(n+\alpha+1)}{\Gamma(n+1)} \frac{2}{[(\nu/2)\cos(\theta)]^\alpha} \frac{\sin(\Theta)}{[\pi\nu\sin(2\theta)]^{\frac{1}{2}}} \quad , \tag{F-3}$$

where

$$x = \nu\cos^2(\theta)\,, \qquad 0 < \theta < \pi/2\,, \qquad 4\Theta(x) = \nu(2\theta - \sin(2\theta)) + \pi \quad . \tag{F-4}$$

One can find similar asymptotic expansions for $e^{-x/2}L_n^\alpha(x)$ at the transition point between the oscillatory and the monotonic regions, $x \simeq \nu$, as well as in the monotonic region, $x > \nu$ [76]. Because, for $\nu \to \infty$, both regions give vanishing contributions to the calculated physical quantities in this thesis, we only state the asymptotics in these regions briefly: In the monotonic region $x > \nu$, the function $e^{-x/2}L_n^\alpha(x)$ behaves asymptotically as $e^{-\Theta'_n}$ with $\Theta'_n = \nu(\sinh(2\theta'_n) - 2\theta'_n)$ and $x = \nu\cosh^2(\theta'_n)$, $\theta'_n > 0$ [76]. Furthermore, one can show that both asymptotic expansions (i.e. the one for the oscillatory region as well as the one for the monotonic region), are valid at the transition point $x \simeq \nu$ except in the range $|x - \nu| < \nu^{1/3}$.

## F.2 Evaluation of the Difference of Vertex Overlaps

With the help of the above asymptotic expansions of the Laguerre polynomials, we obtain for the difference of the vertex overlaps $\mathcal{L}_\sigma^j$ introduced in Eq. (7.6)

$$\mathcal{L}_1^1 - \mathcal{L}_0^1 \approx J_0(qR_c)\left\{J_1\left(qR_c\left[1-\frac{1}{4N}\right]\right) - J_1(qR_c)\right\} \quad . \tag{F-5}$$

Here, it has been assumed that $(q\ell_B)^2 \ll N^{1/3}$. By using the expansion

$$J_1\left(qR_c\left[1-\frac{1}{4N}\right]\right) \approx J_1(qR_c) - \frac{q\ell_B^2}{2R_c}J_0(qR_c) \tag{F-6}$$

and the asymptote

$$J_0^2(qR_c) \sim \frac{1}{qR_c} \quad , \tag{F-7}$$

valid for $qR_c \gg 1$ (i.e., in the ballistic limit under study), we find that the contribution $\mathbf{\Gamma}^{(q/k_F)}$ is negligible with respect to $\mathbf{\Gamma}^{(1/qR_c)}$ whenever $(q\ell_B)^2 \ll 1$.

Due to the asymptotic expansions of the Laguerre polynomials, we find for the momentum region $(q\ell_B)^2 \gg N^{1/3}$

$$\mathbf{\Gamma}^{(q/k_F)} \gg \mathbf{\Gamma}^{(\Delta/\omega_c)}$$

and

$$\mathbf{\Gamma}^{(q/k_F)} \gg \mathbf{\Gamma}^{(1/qR_c)} \quad ,$$

where $1/N, \Delta/\omega_c \ll 1$ has been assumed.